Development of Heterogeneity near the Glass Transition: Phenyl-Ring-Flip Motions in Polystyrene

Bart Vorselaars,*,† Alexey V. Lyulin,†,‡ and M. A. J. Michels†,‡

Group Polymer Physics and Eindhoven Polymer Laboratories, Technische Universiteit Eindhoven, P.O. Box 513, 5600 MB Eindhoven, The Netherlands, and Dutch Polymer Institute, Eindhoven, The Netherlands

Received March 20, 2007; Revised Manuscript Received June 1, 2007

ABSTRACT: Molecular dynamics simulations are employed to study the phenyl-ring flip in polystyrene, thought to be the molecular origin of the γ-relaxation. The results show that upon cooling the system toward the glass transition the motion of the phenyl ring becomes more heterogeneous, which seems to result from a distribution of local energy barriers in combination with slower transitions between states with these local energy barriers. The growing of the heterogeneity affects the determination of the effective energy barrier. In particular, the "static" energy barrier (as determined from the distribution of the orientation of the phenyl ring with respect to the backbone) is found to be different from the "dynamic" energy barrier, as determined from the temperature dependence of some relaxation time (i.e., the activation energy). However, below the glass transition temperature it appears that the two methods render the same value for the height of the energy barrier, although the time scales differ approximately by a constant factor. It is shown that another relaxation time can be determined to characterize the ring-flip process, which seems not to be affected by the growth of heterogeneity and which closely follows the "static" energy barrier. The effective barrier as determined in this way by the simulations is in fair agreement with experimental values for the γ-relaxation.

1. Introduction

The mechanical properties of glassy polymers are complex functions of temperature and experimental time scale. Various relaxation processes determine the precise viscoelastic behavior of a polymer glass, such as chain relaxation, segmental relaxation within a chain, and conformational transitions. The complex microstructure of a polymer material is responsible for the nature and time scales of these relaxation processes. Yet, some generic features are present, related to the physics of the glass transition. The main relaxation process, the α-process, freezes in at the glass-transition temperature T_g. In general, the α-process is a very collective process,[1] which shows strongly non-Arrhenius behavior. Below T_g only local rearrangements of chain segments within their cages formed by neighboring segments are possible. In order of freezing-in upon cooling these sub-T_g processes are called β, γ, ... These faster processes are more Arrhenius-like and less collective in the glassy regime.[1]

An attractive prototype glassy polymer to study experimentally and theoretically is atactic polystyrene (PS). The major reasons for this are that its properties are well documented, it is a common plastic, and its mechanical behavior is still poorly understood, despite the extensive studies of the relaxation processes of PS. The temperature at which the α-relaxation reaches 100 s (which can be used as the definition of the glass-transition temperature[1]) is $T_g \approx 374$ K; the exact value depends on cooling rate and molecular weight distribution.[2]

The β-process (not to be confused with the β-relaxation in the mode-coupling theory (MCT) of the glass transition, of which the time scale diverges near the critical temperature in the ideal-MCT framework[1]) appears for atactic polystyrene around a frequency of 110 Hz at $T = 320$ K; it has an activation energy of about 1.3×10^2 kJ mol^{-1}.[3] At high frequencies the peak of the β-process will merge with the α-relaxation peak.[3] It is believed that the β-process in PS originates from a local oscillation mode of the backbone chain.[3] If annealing conditions are varied, the barrier will also vary between ∼90 and ∼170 kJ mol^{-1}.[4]

The γ-process has a smaller activation energy and has been associated with a phenyl-ring flip. The activation energy obtained by mechanical experiments is 34−38 kJ mol^{-1}.[3,5] Other experimental studies[6] lead to energy barrier heights in the range 21−29 kJ mol^{-1}; in these studies the energy barrier was determined by a fit based on a rotator model, leading to a lower energy value than obtained from an Arrhenius fit.

As the ascribed molecular origin of the γ-relaxation is conceptually simple, it has been subject of many theoretical studies. Early estimates for the energy barrier of a phenyl-ring flip are based on taking into account only intrachain interactions.[6−10] It was found that the potential energy barrier depends on the conformation of the backbone chain and on tacticity.[7−9] The energy barrier is lower when the backbone torsions operate cooperatively with the phenyl-ring motion.[8,10]

However, in a melt the backbone dihedral angles cannot rotate freely, without hindering other chains as well. When other chains are also included (i.e., a phenyl-ring flip in its glassy neighborhood), the mean energy barrier height determined by an energy minimization method turns out to be 116 kJ mol^{-1}.[11] The actual distribution of barrier heights was found to be very broad, in the range of 0.96−1115 kJ mol^{-1} (for the cases in which the energetic barrier was positive). Another study[12] also uses a form of energy minimization to determine energy barriers in the glassy structure. The result ranges from 19.2 to 133 kJ mol^{-1} for 10 different measurements of a phenyl-ring rotation (in which rotations in both directions have been considered, viz. clockwise and counterclockwise). These results show that the glassy structure has a tremendous effect on the actual barrier of the phenyl-ring flip. So the relaxation of the surrounding polymer

* To whom correspondence should be addressed. E-mail: B.Vorselaars@tue.nl.
† Technische Universiteit Eindhoven.
‡ Dutch Polymer Institute.

10.1021/ma070669r CCC: $37.00
Published on Web 07/12/2007

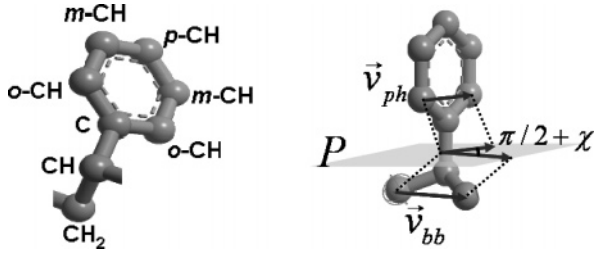

Figure 1. (left) Monomer unit of the polystyrene model with the naming convention of the (united) atoms. Here o = ortho, m = meta, and p = para. The notation x-CH is used for any of the three possible positions of the CH group in the phenyl ring. (right) Illustration with the definition of the angle χ between the phenyl ring and the backbone. See text for details.

matrix should be taken into account for studying the dynamical behavior of the phenyl ring. Variations in molecular packing can cause a distribution of relaxation times, which in turn can cause heterogeneous dynamics.[13]

The usage of molecular dynamics (MD) simulations is an effective method to study the dynamics of transitions of small chemical groups near the glass transition. The results of previous MD simulations for melts of other polymer systems have shown that there is a distribution of transition rates for the rotation of a side group (such as for the rotation of the methyl group in poly(methyl methacrylate),[14] in poly(vinyl methyl ether) (PVME),[15] and in polyisobutylene[16]) or for conformational transitions.[17] Also, a distribution of energy barrier heights has been found for CH_3 rotations in PVME[18] or for conformational transitions.[17] MD simulations have been carried out before for polystyrene as well,[19−35] and some of these simulation results have been used to look at typical relaxation times in the vicinity of the glassy state.[25,28,30,33] However, no emphasis was given to the motion of a phenyl ring.

The aim of the present paper is to study the flip of the side-group phenyl ring in a melt of atactic polystyrene and determine the accompanying energy barrier landscape, typical relaxation time scales, and the Arrhenius activation energy by means of different methods. A special point of focus is to look at the influence of the glassy dynamics on the dynamical properties of this ring, which effectively makes the ring flip very heterogeneous (in terms of a wide distribution of relaxation times).

The paper is organized as follows. In the next section, the polystyrene model is described and simulation details are explained. From MD simulation data the free energy barrier for the phenyl-ring flip is then determined, by means of the distribution function of the orientation of the phenyl ring with respect to the backbone. Next the temperature dependencies of the relaxation times of autocorrelation functions are studied to yield a value for the activation energy. Van Hove functions are analyzed for studying the heterogeneity in the dynamical behavior of the phenyl ring, leading to a kinetic model for ring flipping. Finally, some conclusions are stated.

2. System Description and Simulation Details

The atactic-polystyrene melt in the simulation consists of 8 chains of 80 monomers each. In the left panel of Figure 1 a monomer unit of polystyrene is depicted together with the nomenclature of the (united) atoms. The united-atom force field is described in Table 1. Simulations are carried out in the constant-*NPT* ensemble (constant number of particles *N*, pressure *P*, and temperature *T*), using velocity Verlet as the numerical integration scheme for the Newtonian equations of motion (with an integration time step of 4 fs), the Berendsen barostat[36] (τ_P = 10 ps), and the collisional dynamics method[37] as a thermostat (λ = 1 ps^{-1}, m_0 = 0.1 Da). Strictly speaking, when using the Berendsen barostat, the constant-*NPT* ensemble is not probed,[36] but this effect is assumed to be of minor significance for the present study.

Table 1. United-Atom Force Field in Use for Atactic Polystyrene[a]

nonbonded interaction[b]
$U_{LJ}(r) = \epsilon_{ij}[((\sigma_{ij}/r))^{12} - 2((\sigma_{ij}/r))^6]$, $\epsilon_{ij} = \sqrt{\epsilon_i \epsilon_j}$,
$\sigma_{ij} = {}^1/_2(\sigma_i + \sigma_j)$
ϵ = 0.377 kJ mol^{-1}, σ = 4.153 Å for CH
ϵ = 0.502 kJ mol^{-1}, σ = 4.321 Å for CH_2
ϵ = 0.502 kJ mol^{-1}, σ = 4.153 Å for C and x-CH
bond stretching
$U_l(l) = k_l(l - l_0)^2$
k_l = 669 kJ mol^{-1} Å^{-2}, l_0 = 1.53 Å for CH_2−CH
k_l = 669 kJ mol^{-1} Å^{-2}, l_0 = 1.51 Å for CH−C
k_l = 669 kJ mol^{-1} Å^{-2}, l_0 = 1.40 Å for C−x-CH
k_l = 669 kJ mol^{-1} Å^{-2}, l_0 = 1.40 Å for x-CH−x-CH
bond angle
$U_\theta(\theta) = k_\theta(\theta - \theta_0)^2$
k_θ = 251 kJ mol^{-1} rad^{-2}, θ_0 = 109.5° for X−CH−X
k_θ = 264 kJ mol^{-1} rad^{-2}, θ_0 = 109.5° for X−CH_2−X
k_θ = 293 kJ mol^{-1} rad^{-2}, θ_0 = 120.0° for X−C−X and X−x-CH−X
torsion
$U_\varphi(\varphi) = k_\varphi \cos(n\varphi)$
k_φ = 2.93 kJ mol^{-1}, n = 3 for X−CH−CH_2−X
k_φ = 2.09 kJ mol^{-1}, n = 2 for X−CH−C−X
k_φ = −27.2 kJ mol^{-1}, n = 2 for X−C−x-CH−X
k_φ = −54.4 kJ mol^{-1}, n = 2 for X−x-CH−x-CH−X
improper torsion[c]
$U_{\varphi'}(\varphi) = k'_\varphi \cos(n\varphi')$
$k_{\varphi'}$ = 20.9 kJ mol^{-1} , n = 2 for X−C−X−X′
$k_{\varphi'}$ = 20.9 kJ mol^{-1} , n = 3 for X−CH−X−X′

[a] It is based on the united-atom force field as being used by ref 19, and the notation in use is similar. The ratio of number of meso to the number of racemic dyads is near unity. Differences in the force field are that the bonds and the valence angles in the phenyl ring are flexible, the planarity of the phenyl ring is accomplished as is done by ref 23, and tacticity of the chain is accomplished by a different improper torsion potential. The parameters for the CH_3 united atoms positioned at the chain ends are the same as for CH_2. The mass m of each (united) atom is calculated using m_C = 12 Da and m_H = 1 Da. The X stands for the (united) atom having a chemical bond with the (united) atom next to it. [b] Lennard-Jones (LJ) interactions are only not taken into account for particles which are separated by one or two chemical bonds. A so-called switching function[39] was used to smoothly cuto the LJ potential at large distances with $R_{on} = 2\sigma_{ij}$ and $R_{off} = 2.2\sigma_{ij}$. [c] The first improper torsion is used for keeping the *o*-CH, C, and CH group in a plane. The second one is used for maintaining the tacticity of the chain. The four consecutive (united) atoms defining the improper torsion are for the (united) atoms around the CH united atom (X−CH−X−X′) C−CH−CH_2−CH_2, CH_2−CH−CH_2−C, and CH_2−CH−C−CH_2 and for the united atoms around the C atom (X−C−X−X′) x-CH−C−x-CH−CH, x-CH−C−CH−x-CH, and CH−C−x-CH−x-CH. It is called improper, as there is no direct chemical bond between the third and fourth (united) atom defining the torsion.

The sample is prepared by a procedure similar to that of ref 27, starting with a one-chain melt of polystyrene. After the equilibration of this single chain, the orthorhombic box is doubled in all three directions, and the resulting sample is equilibrated further for another 10 ns at T = 540 K. To correct for the potential cutoff and any other force field deviations, the pressure has been adjusted so that the density at T = 540 K equals the experimentally observed density at this temperature and at atmospheric pressure.[38] The sample is subsequently cooled to the desired temperature by 0.01 K ps^{-1}. This process is done for five independent samples in order to increase statistics. For testing the proper temperature behavior of some of the data, the temperature of one sample (first equilibrated at T = 540 K) has been set to 1000 K, followed by an additional 4 ns equilibration with an integration time step of 2 fs. To see what the influence of the glassy state is compared with the gas phase, another simulation has been carried out, in which only

one chain has been simulated. This atactic polystyrene chain consists of 15 monomer units and is placed in a vacuum.

The glass-transition temperature T_g of this 8-chain model for atactic polystyrene is determined by plotting the specific volume vs temperature and applying a linear fit to both low and high temperatures. The crossing point of these linear fits is then taken as the definition of the glass-transition temperature, with the result $T_g = 388$ K.[29] This is somewhat higher than the experimentally determined glass-transition temperature for approximately the same molecular weight, $T_g = 361-363$ K.[2,38] The difference becomes smaller upon extrapolating the observed glass-transition temperature toward experimental cooling rates.[29]

As the present study is mainly concerned with the rotational dynamics of the phenyl ring, the angle χ between the phenyl ring and the backbone is defined here in detail (see Figure 1). It is slightly different from the one as given in ref 40, as now it is not assumed that the phenyl ring is strictly planar. (In the case of an all-atom model of polystyrene a different convention is possible.[41]) The plane P is defined by the normal vector C−CH connecting the phenyl ring to the backbone. The vector $\mathbf{v}_{ph}$ pointing from one *o*-CH to the other *o*-CH and the vector $\mathbf{v}_{bb}$ pointing from one CH_2 to the other CH_2 (two chemical bonds away) are projected onto this plane P. Then the angle χ is defined as the angle between these two projected vectors minus $\pi/2$. In this way the equilibrium position of the phenyl ring with respect to the backbone is around $\chi = 0$ and around $\chi = \pi$.

3. Results and Discussion

The rotational dynamics of the phenyl ring can be studied in various ways. First the free energy barrier height for rotation is determined from the probability distribution of χ (a measure for the orientation of the phenyl ring with respect to the backbone). As a second method, the time dependence of some autocorrelation functions associated with the phenyl ring is investigated; from this an activation energy can be distilled. The concept of heterogeneity is used to explain the difference between the two energies thus determined. To acquire more evidence for heterogeneous dynamics, some typical trajectories of the phenyl-ring angle with respect to the backbone are displayed, and the self-part of the van Hove function is calculated. Based on this, a two-state model (χ around 0 vs χ around π) is used to calculate in yet another way an activation energy. The various results give clear evidence for heterogeneity in the glassy dynamics.

3.1. Free Energy Barrier. To see what energy barrier is associated with a phenyl flip in our constant-*NPT* simulation run, the distribution function $\rho(\chi)$ has been measured. From this the (Gibbs) free energy $G(\chi)$ can be calculated by using the Boltzmann distribution law[42]

$$\rho(\chi) = \rho(\chi_{min}) \exp\left[-\frac{G(\chi) - G(\chi_{min})}{k_B T}\right] \qquad (1)$$

with k_B Boltzmann's constant. The reference value χ_{min} is taken to be the value of χ at which the free energy is at its minimum. A similar analysis has also been carried out in ref 18. The result is shown in Figure 2 for two different temperatures. Data for other temperatures are similar. The shape of this effective potential (potential of mean force) is well described by a simple cosine function

$$G(\chi) - G(\chi_{min}) = \frac{1}{2}\Delta G_{max}(1 - \cos(\chi)) \qquad (2)$$

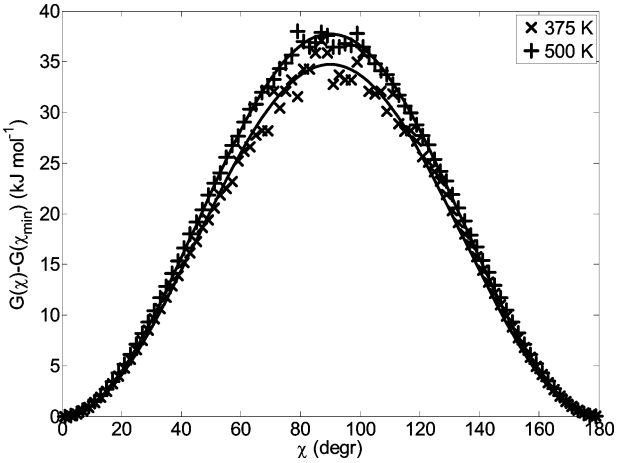

Figure 2. Free energy G for two different temperatures (around T_g and well above it) as a function of the angle χ of the phenyl ring with respect to the backbone, as calculated using eq 1. Solid lines are fits to the simulation data (crosses and pluses) with the cosine function eq 2.

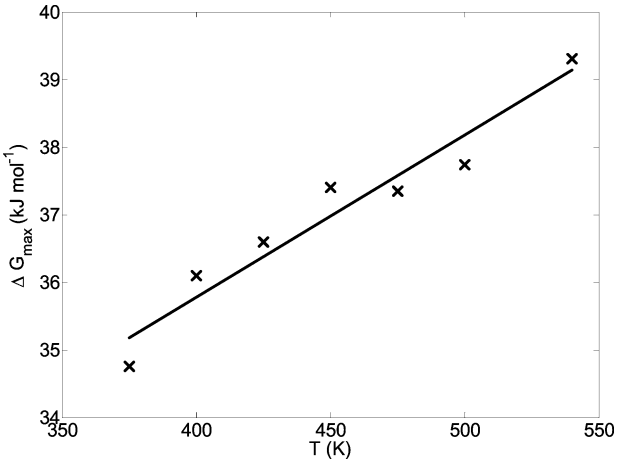

Figure 3. Free energy barrier height as a function of the temperature, extracted from the distribution function of χ, eq 1. Solid line is a fit to the simulation data (crosses) with eq 3.

with ΔG_{max} the free energy barrier height. This barrier height ΔG_{max} as acquired by fitting $G(\chi) - G(\chi_{min})$ by eq 2 is plotted in Figure 3 as a function of temperature.

The entropic part of the free energy barrier height can be determined by fitting the data with the linear relation

$$\Delta G_{max}(T) = \Delta H_{max} - T\Delta S_{max} \qquad (3)$$

when one assumes that the enthalpy difference ΔH_{max} and the entropy difference ΔS_{max} are independent of temperature. The contribution $P\Delta V_{max}$ to the free energy barrier could also be determined by varying the pressure, but it is assumed that this contribution is temperature-independent as well and therefore it is discarded in this study. In this way ΔH_{max} could be interpreted as some kind of activation enthalpy, in the case of a single barrier (see, e.g., ref 43). The outcome of the fit is $\Delta H_{max} = 26$ kJ mol^{-1} and $\Delta S_{max} = -0.024$ kJ mol^{-1} K^{-1} (Figure 3). The free energy barrier height is seen to increase with increasing temperature. This could be interpreted that it is entropically unfavorable to be at the unstable maximum position ($\chi_{max} = \pi/2$), compared to the stable minimum position ($\chi_{min} = 0$).

The entropic contribution to the free energy barrier height is higher than found from an energy-minimization technique.[12] From our simulation results the contribution $T\Delta S_{max}$ to the free

energy barrier at $T = 300$ K is estimated to be about 20%. The contribution $T\Delta S_{max}$ obtained from the energy minimization, in which the entropy is acquired by applying a quadratic approximation for the potential energy surface near the transition state for a phenyl-ring flip, was less than 10%.[12]

Another way to determine the energetic barrier is by looking at the temperature dependence of the relaxation times. In the next section relaxation times associated with a phenyl-ring flip are calculated; afterward, activation energies corresponding to some of these times are determined.

3.2. Time Correlation Functions. The dynamics of the phenyl ring is examined by looking at the vector connecting the two united carbon atoms in the ortho position, *o*-CH (see Figure 1). The rotational behavior of this vector $\mathbf{v}_{ph}$ can be studied by considering ensemble-averaged Legendre polynomials $P_l(x)$ of the inner product of the unit vector $\hat{\mathbf{v}}_{ph} \equiv \mathbf{v}_{ph}/|\mathbf{v}_{ph}|$ at time t_0 with itself at time $t_0 + t$, i.e., the autocorrelation function

$$C_l(t) = \langle P_l[\hat{\mathbf{v}}_{ph}(t_0)\cdot\hat{\mathbf{v}}_{ph}(t_0 + t)]\rangle \tag{4}$$

One of the reasons to look at this quantity is that some of these autocorrelation functions can be measured experimentally. In particular, when instead a C−H vector is considered, then the correlation time (also called an average relaxation time[1])

$$\tau_c \equiv \int_0^\infty ACF(t)\, dt \tag{5}$$

is measurable by NMR experiments, if $ACF(t) = C_2(t)$. Reasonable agreement was observed when comparing the result of this kind of NMR experiments to the results of MD simulations.[30]

It is quite common when studying glassy materials to fit such autocorrelation functions by a Kohlrausch−Williams−Watts (KWW) stretched-exponential function[1]

$$A \exp[-(t/\tau_{KWW})^\beta] \tag{6}$$

in which τ_{KWW} is a typical time scale of relaxation, β the stretch exponent, and A a preexponential factor to account for other relaxation processes at shorter time scales (such as librating motion, which usually occurs at time scales below 4 ps, the interval at which trajectories are saved in this study). Integrating eq 6[44] then results in the correlation time τ_c (eq 5)

$$\tau_c = \frac{\tau_{KWW}}{\beta}\Gamma(\beta^{-1}) \tag{7}$$

with $\Gamma(x)$ the (complete) gamma function. So for $1 \geq \beta \geq {}^1/_2$ the correlation time τ_c is at most a factor of 2 larger than τ_{KWW}. The KWW function can be considered as arising from a specific superposition of exponentials

$$\exp[-(t/\tau_{KWW})^\beta] = \int_0^\infty \rho_{KWW}(\tau) \exp\left(-\frac{t}{\tau}\right) d\tau \tag{8}$$

with the KWW distribution function $\rho_{KWW}(\tau)$. The width of $\rho_{KWW}(\tau)$ is then determined by the exponent β, a lower value of β meaning a wider distribution.[44]

One should be cautious in interpreting the fitting parameters of the KWW function. A limited time window for the relaxation function (due to limitations in simulation time) can result in a lower value for the fitted τ_{KWW}.[45] Also, in the case of glasses the interference of the start of the α-relaxation with the end of the cage plateau can result in lower values of β.[46]

The results for

$$C_1(t) = \langle \hat{\mathbf{v}}_{ph}(t_0)\cdot\hat{\mathbf{v}}_{ph}(t_0 + t)\rangle \tag{9}$$

and

$$C_2(t) = \frac{3}{2}\langle[\hat{\mathbf{v}}_{ph}(t_0)\cdot\hat{\mathbf{v}}_{ph}(t_0 + t)]^2\rangle - \frac{1}{2} \tag{10}$$

describing the reorientation of the normalized *o*-CH−*o*-CH vector are shown in Figure 4. It is seen that the three-parameter KWW function is able to describe the data well.

Some important differences can be observed when comparing the $C_1(t)$ and $C_2(t)$ autocorrelation functions for the *o*-CH−*o*-CH phenyl vector. In Figure 5 the correlation time (deduced from eqs 6 and 7) is plotted as a function of temperature. The relaxation time of $C_2(t)$, τ_{C_2}, rises more quickly than the one of $C_1(t)$, τ_{C_1}, upon decreasing temperature. This is because $C_2(t)$ is invariant under a phenyl-ring flip. So a flip contributes to the relaxation of $C_1(t)$, but not of $C_2(t)$. Nevertheless, $C_2(t)$ still relaxes at low temperatures. This means that main-chain reorientation and/or the flapping motion of the phenyl ring around the backbone still are active relaxation modes at low temperatures, although much slower than the motion of the phenyl-ring flip itself.

To isolate the pure effect of the phenyl-ring reorientation with respect to the backbone, we consider the relaxation of the autocorrelation function of the cosine of the accompanying angle χ (Figure 1)

$$C_\chi(t) = \langle\cos[\chi(t) - \chi(0)]\rangle \tag{11}$$

This autocorrelation function would be identical to $C_1(t)$ (eq 9), if the backbone would be frozen and the phenyl ring could only move by rotating around the chemical bond joining it to the backbone. It turns out that this is almost the case for low temperatures, where the two autocorrelation functions are close to each other. The time dependence of $C_\chi(t)$ is also well-described by a stretched-exponential function, eq 6. The temperature dependence of the corresponding correlation time $\tau_{C\chi}$ is shown in Figure 5. At high temperature this relaxation is rather slow, slower than both $C_1(t)$ and $C_2(t)$. This is because both $C_1(t)$ and $C_2(t)$ are able to relax by the motion of the backbone, while $C_\chi(t)$ can only relax via the relative motion of the phenyl ring with respect to the backbone. However, upon decreasing the temperature, this behavior changes. The flip-relaxation channel becomes the dominant one for temperatures of about 440 K and lower, as then the relaxation time of $C_1(t)$ almost equals that of $C_\chi(t)$, $\tau_{C\chi}$. So the difference between $C_1(t)$ and $C_2(t)$ is due to the (obvious) anisotropy of the relaxation; for low temperatures it is for example easier for the phenyl ring to make a π-flip motion around its axis than to end up with a $\pi/2$ rotation around the same axis (not rotation invariant in χ) or to rotate around a different axis (anisotropic in the orientation of the axis). Anisotropic relaxations have been studied before for other polymer systems as well.[47,48]

Despite the dominance of the flip-relaxation channel at lower temperatures, it seems that for temperatures below about 420 K the three different relaxation times show approximately the same temperature dependence (see Figure 5). This observation could be an indication of a coupling between the backbone conformation and the rotation of the phenyl ring. An analogous coupling was also found for a different polymer system.[16] In ref 7 it is shown that the energy barrier for a phenyl-ring flip can exceed 400 kJ mol^{-1} for some accompanying backbone conformations. A change to a new backbone conformation with

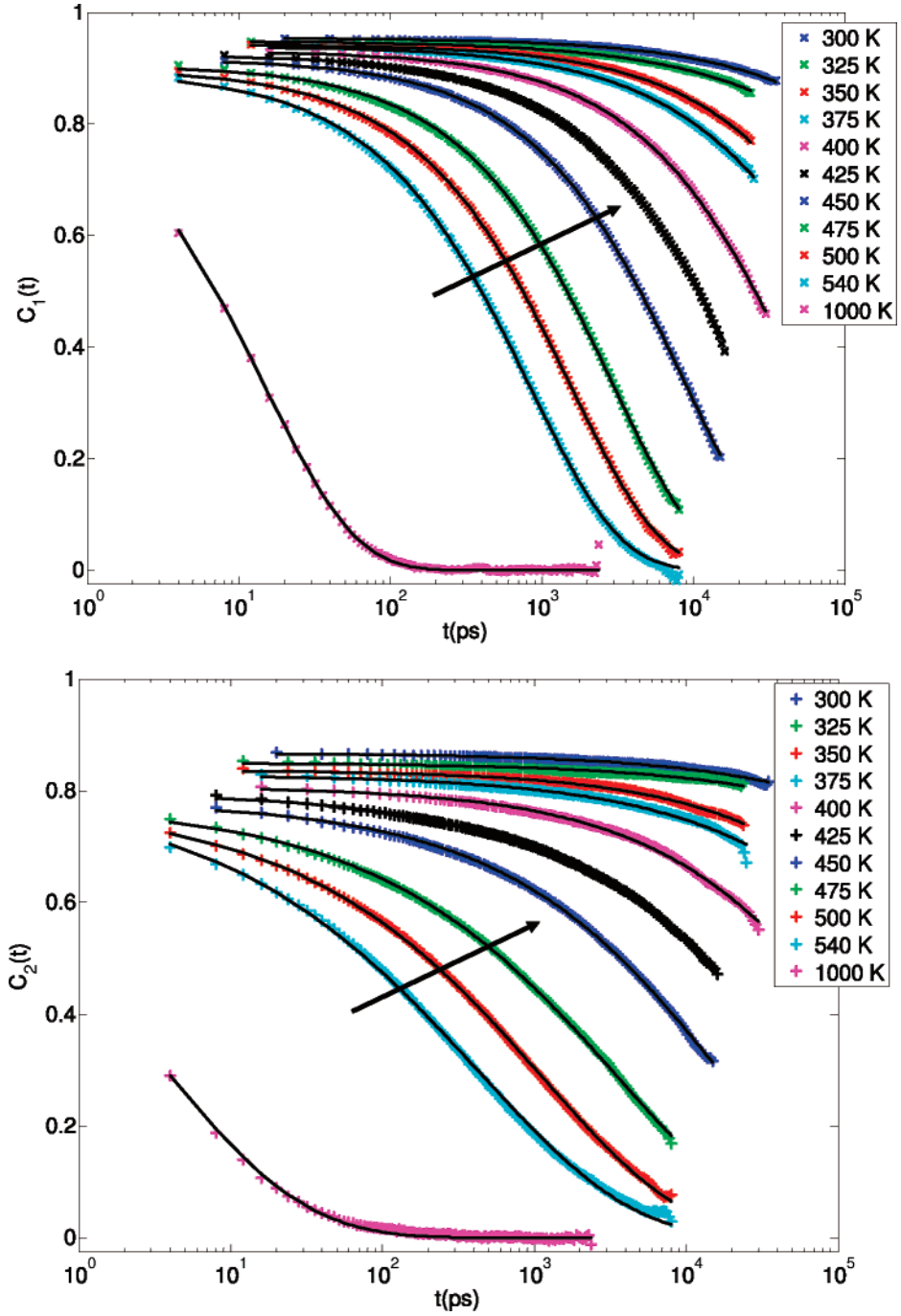

Figure 4. $C_1(t)$ and $C_2(t)$ for the vector $\mathbf{v}_{ph}$ pointing from one *o*-CH atom to the other one within a phenyl ring for various temperatures. Solid lines are fits to the simulation data by a stretched exponential, eq 6. Arrows point toward relaxation curves of decreasing temperature.

a lower energy barrier for the phenyl-ring flip would allow these phenyl rings to flip much earlier. As $C_2(t)$ is invariant under a phenyl-ring flip, its long-time behavior is mostly sensitive to backbone relaxations. Therefore, a plausible explanation for the observation that the temperature dependencies of the different relaxations times are about equal for low temperatures is that the relaxation of the phenyl rings which have a high-barrier conformation for a flip have to wait for the relaxation of the backbone.

3.3. Activation Energy from Relaxation Times. In section 3.1 the free energy barrier height for a phenyl-ring flip was determined by considering the distribution function of the angle χ (Figure 3). Alternatively, one can determine the activation barrier (i.e., the barrier to activate the motion of the process) by assuming that the relaxation time of $C_\chi(t)$ follows activated kinetics (Arrhenius-like behavior)

$$\tau = \tau_0 \exp\left(\frac{\Delta H}{k_B T}\right) \tag{12}$$

in which the inverse of the preexponential factor τ_0^{-1} is a measure for the attempt rate[43] and ΔH is the activation enthalpy. The choice of activated behavior might be motivated by the experimental observation that secondary relaxations are usually well described by such a law,[1] including the γ-relaxation of polystyrene.[3] This in contrast with the main α relaxation, which is usually described by the Vogel−Fulcher−Tamman equation.[1] The Arrhenius fit of the relaxation times of $C_\chi(t)$ results in an activation enthalpy of 50 kJ mol^{-1} for the temperature range of

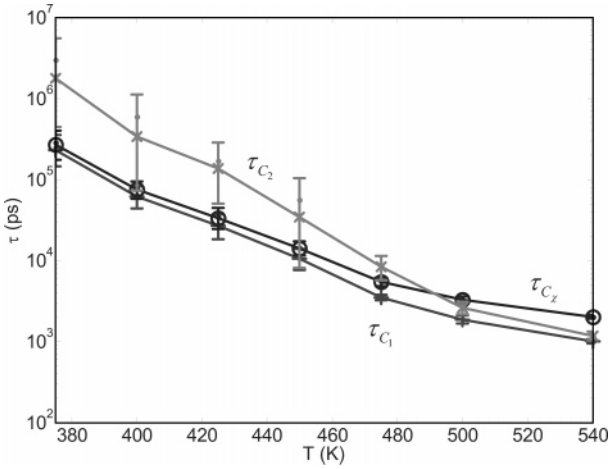

Figure 5. Correlation relaxation times as a function of temperature for the vector within the phenyl ring (τ_{C_1} (pluses) as determined by fitting $C_1(t)$ and τ_{C_2} (crosses) by fitting $C_2(t)$ depicted in Figure 4 by eq 6) and for the χ angle (τ_{C_χ} (circles) by fitting $C_\chi(t)$ (eq 11) by eq 6). All KWW times are rewritten in a correlation time by using eq 7. Solid lines serve as a guide to the eye.

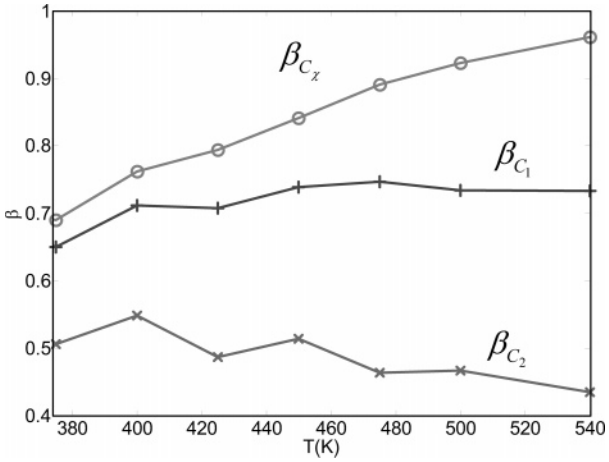

Figure 6. Fitted KWW exponent β as a function of temperature for (+) the relaxation of the *o*-CH−*o*-CH vector within the phenyl as probed by $C_1(t)$, (×) same, now as probed by $C_2(t)$, and (○) the relaxation of the χ angle as probed by the accompanying angle-based $C_\chi(t)$. Solid lines serve as a guide to the eye.

375−540 K. However, fitting the results for the temperature range below the glass-transition temperature, 300−375 K, results in a lower activation enthalpy, 35 kJ mol^{-1}.

So the activation enthalpy as acquired by an Arrhenius plot of τ_{C_χ} for T in the range 375−540 K is almost twice the enthalpy barrier height as determined from the distribution function $\rho(\chi)$, which was $\Delta H_{max} = 26$ kJ mol^{-1}. From one point of view a different value is what one would expect. The decorrelation of $C_\chi(t)$ is described by a stretched-exponential fit, with the temperature-dependent KWW exponent β_{C_χ} found to be smaller than 1. As discussed, this implies a distribution of relaxation times $\rho(\tau) \approx \rho_{KWW}(\tau)$ rather than a single transition time. Another way of interpreting this is that there exists a distribution of energy barrier heights, which obviously determines the average energy barrier. One reason for this fluctuating barrier height could be the cooperative nature of the flip transition, as shown by energy-minimization methods.[8,10,12] The energy barriers for some conformations are much lower than for other ones. Also, the local barrier heavily depends on the nonbonded local environment, i.e., on the interchain interactions.[11,12]

In Figure 6 the KWW exponent β of various autocorrelation functions is plotted as a function of temperature. At relatively high temperature $\beta_{C_\chi} \approx 1$. This is what one would expect for a relaxation mechanism which only involves a single energy barrier. So this indicates that at these temperatures the phenyl-ring flip might be approximately described by a single barrier, too.

At lower temperature β_{C_χ} decreases. One way of interpreting this is that the distribution of energy barriers becomes broader upon lowering the temperature. However, then the question remains regarding the origin of the broadening of this distribution. A more appealing interpretation is that a set of states with a diversity in energy barriers exists both at low and at high temperatures. Only now the difference is that upon lowering the temperature the residence time at each state (with accompanying energy barrier) increases, making it harder to find the lowest energy barrier within the typical time of a transition. This state is likely to be largely characterized by the backbone conformation, which mainly determines the potential energy barrier of a phenyl-ring flip (as is discussed before). The relaxation of the backbone is then indicative of the residence time at each state. This interpretation is supported by the simulation result of the atactic chain of polystyrene in vacuum at $T = 375$ K. For this simulation $\beta_{C_\chi} = 1$ (compared to $\beta_{C_\chi} = 0.7$ for the glassy system at the same temperature). In a vacuum conformational transitions are not hindered by the presence of other chains, leading (in this picture) to faster transitions between the various local energy barriers, and thereby the phenyl ring with its surroundings (apparently) finds the lower energy barrier within the transition time accompanied by this energy barrier.

A decrease of the stretch parameter β for decreasing temperature has been observed for other glassy materials as well, such as for the autocorrelation function of the torsion angle in polyethylene.[49]

In contrast to β_{C_χ}, β_{C_2} is approximately independent of temperature (although a small drift toward higher values upon cooling is visible, which possibly originates from the limited time window available for fitting; it is known that in some situations this could lead to an increase in the fitted stretch parameter β[55]) and approximately equal to 0.4−0.6. This value is typical for simulation results of polymers. It has been observed in other MD simulations of polystyrene,[30] and also for other polymers, such as poly(ethylene oxide).[48]

3.4. Heterogeneity. A distribution of energy barrier heights generally would imply heterogeneous dynamics. This can indeed be seen from trajectories of the χ angle. Some typical trajectories are shown in Figure 7. For $T = 300$ K it is observed that out of a total number of 560 phenyl rings (the five phenyl rings near each chain end are discarded in view of the known increase in mobility around the ends of a polymer chain[27,50]) 548 phenyl rings (98%) did not flip at all during a 24 ns simulation run. However, it turns out that of the remaining phenyl rings eight flipped once, two flipped twice, and two flipped more than 10 times, illustrating the nonhomogeneous dynamics during this time window.

It is also observed that, while the averaged equilibrium position of the χ angle is at 0 (and at π), some phenyl rings seem to prefer other (temporarily) quasi-equilibrium positions (such as seen in Figure 7b,c) and that infrequent transitions are possible between these quasi-equilibrium positions (Figure 7c). Note also that a phenyl-ring flip not necessarily forces the quasi-equilibrium position to change (Figure 7b). So next to the heterogeneity in energy barrier heights, there also exists heterogeneity in the value of χ_{min}, i.e., in the angle χ at which the energy is at its minimum. Yet another type of heterogeneity

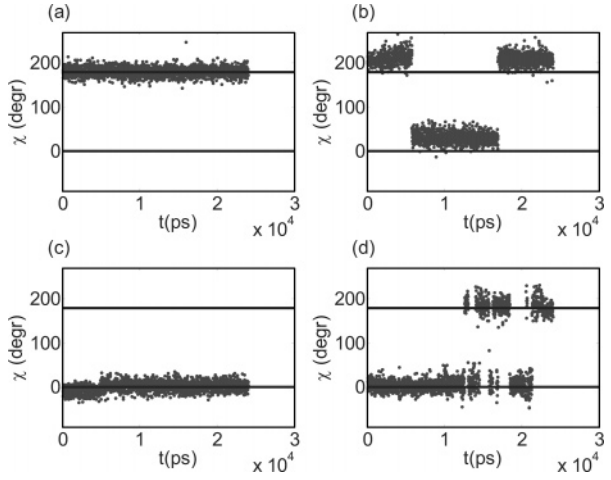

Figure 7. Typical trajectories for the χ angle at $T = 300$ K during a 24 ns simulation run (χ values are plotted every 12 ps): (a) no jumps, (b) two jumps, (c) jump within cage around 5 ns, (d) many jumps. Solid lines denote the equilibrium values $\chi_{min} = 0, \pi$.

is in the width of the energy minimum. The fluctuations around the local minimum in Figure 7b are significantly larger than for example those in Figure 7a. These small-scale heterogeneities can be seen more quantitatively by looking at the van Hove function, which is carried out in the next section.

As was concluded from the behavior of the time correlation functions, the reason for these heterogeneities must be sought in a combination of inter- and intrachain interactions. For example, a shift of the equilibrium position to a new quasi-equilibrium position could arise because of these interactions, which could effectively hinder the phenyl ring to be around the usual equilibrium position, as has been illustrated in ref 51. Of course, some types of heterogeneities already exists in the sample. The polystyrene chains are atactic; three different triads for a phenyl ring are present in the simulation run (meso, racemic, and hetero). Also, the presence of chain ends near a phenyl ring could be a reason for a variation in the environment. The two most active phenyl rings in this particular trajectory (which turn out to be well separated from each other, namely about 30 Å) are in a different type of triad, and the closest chain ends have a minimal separation of about 3.2 and 7.5 Å for these phenyl rings. Moreover, all three types of triads are among the phenyl rings which flip two or more times. On the basis of these results, no definite conclusions can be drawn whether or not the dynamical heterogeneities of the phenyl-ring flip are mainly caused by the presence of chain ends or due to variations in tacticity.

As mentioned before, a plausible cause of the heterogeneity is that below the glass-transition temperature the motion of the main chain is nearly frozen in, so is the backbone conformation near a phenyl ring. In refs 7−9 it has been shown that some backbone conformations (depending on the type of triad) result in a lower energy barrier for the phenyl-ring flip than other backbone conformations. At sufficient low temperature some phenyl rings can therefore be stuck in these low-energy-barrier conformations, while others are stuck in the high-energy-barrier conformations. From this one could conclude that the length scale associated with the most active phenyl rings is limited to one phenyl ring only, as each phenyl ring is surrounded by its own backbone conformation. It would be interesting to have a future study investigating the correlations between active phenyl rings and specific backbone conformations by means of molecular dynamics simulations, as is, e.g., done in the study of methyl group rotations in polyisobutylene.[16]

3.5. Van Hove Function. The self-part of the van Hove function[52] can be examined to give more insight into the distribution of angular displacements over a time interval t of the angle χ_i describing the orientation of a phenyl ring i with respect to the backbone. As χ is a periodic coordinate, the periodic, "boxed" van Hove function

$$G_s(\Delta\chi,t) \equiv \langle \delta\{\Delta\chi - |f[\chi_i(t_0 + t) - \chi_i(t_0)]|\}\rangle \qquad (13)$$

is calculated. Here the averaging $\langle\cdots\rangle$ is done over every phenyl ring i as well as over all available time origins t_0. To handle the periodicity of the χ angle, the difference $\chi_i(t_0 + t) - \chi_i(t_0)$ is first boxed (as is also common in calculations of spatial coordinates in combination with periodic boundary conditions[36]) by using the function $f(\chi) \equiv \chi - 2\pi\ \mathrm{anint}[(1/2\pi)\chi]$, in which the function anint(x) rounds x toward the nearest integer. The absolute value symbols, |...|, serve to acquire only positive displacements. So the self-part of the van Hove function $G_s(\Delta\chi,t)$ is a measure for the probability of a certain angular displacement $\Delta\chi$ after a period of time t.

The simulation data of $G_s(\Delta\chi,t)$ for $T = 300$ K are displayed in Figure 8. The first bump at angle differences smaller than about $\pi/2$ is relatively constant over the investigated time interval. This means that the surrounding of the local minimum is already mostly explored within 12 ps. Nevertheless, there is a small increase in the displacement up until about $\Delta\chi = \pi/2$. Probably this has its origin in processes responsible for the small-scale heterogeneity in the value of χ_{min} and in the magnitude of fluctuations around this value. If a phenyl ring makes for example a small-scale jump to a new quasi-equilibrium position (such as the one visible in the trajectory displayed in Figure 7c), then the effective angular displacement within the first cage will increase.

The second bump is representative for the fraction of phenyl rings which made a flip motion. Note that it is steadily increasing in time. The next section will be devoted to the time dependence of this fraction.

3.6. Two-State Analysis. To isolate the fraction of jumped phenyl rings in a more quantitative way, we divide the phenyl rings into two states, ↑ and ↓, in which the boundary between the two states is taken to be at $\chi = 90°$. If a π flip occurs, the phenyl ring will go from one to the other state. A similar analysis for transitions between the trans, gauche$^+$, and gauche$^-$ conformations has been carried out before.[15,53]

The ↑ state is defined so that at $t = 0$ all phenyl rings are in this state. The fraction of phenyl rings at time t in the ↑ state is denoted by $\phi_\uparrow(t)$. The initial conditions are $\phi_\uparrow(0) = 1$ and $\phi_\downarrow(0) = 0$, and it is expected that $\lim_{t\to\infty} \phi_\uparrow(t) = \lim_{t\to\infty} \phi_\downarrow(t) = \phi_{eq} = 1/2$, since the two states are completely symmetric. If there would be only one energy barrier and if inertial effects can be neglected, then at sufficiently low temperatures this process can be modeled by a simple master equation[54]

$$\dot{\phi}_\uparrow(t) = -k\phi_\uparrow(t) + k\phi_\downarrow(t)$$
$$\dot{\phi}_\downarrow(t) = -k\phi_\downarrow(t) + k\phi_\uparrow(t) \qquad (14)$$

with the solution

$$\phi_\uparrow(t) = \frac{1}{2}(1 + e^{-2kt})$$
$$\phi_\downarrow(t) = \frac{1}{2}(1 - e^{-2kt}) \qquad (15)$$

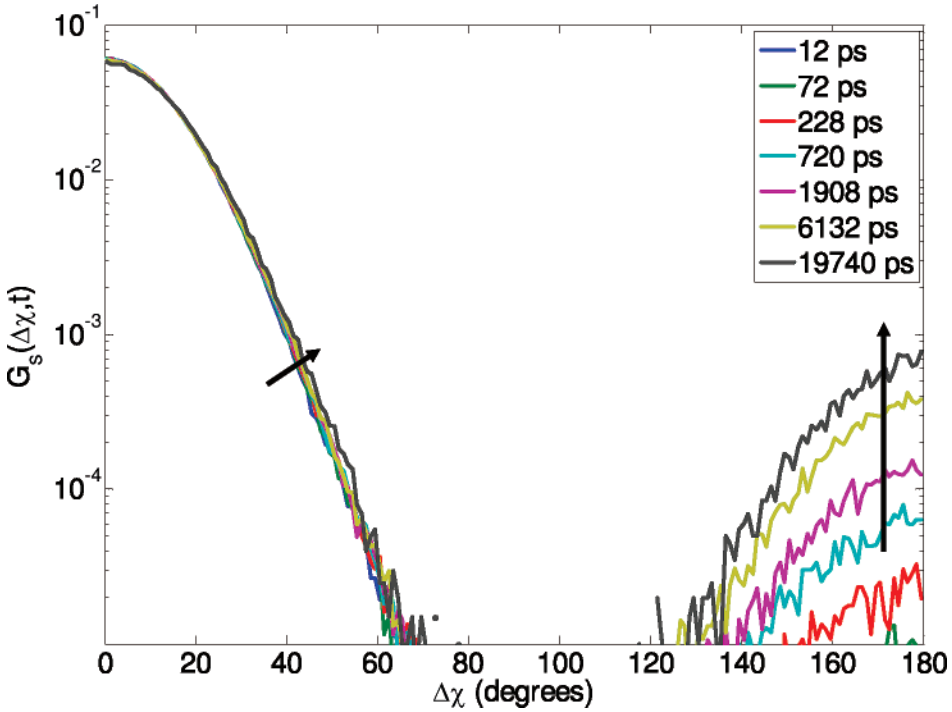

Figure 8. Self-part of the van Hove function $G_s(\Delta\chi,t)$ (eq 13) for the absolute value of the boxed angular displacement $\Delta\chi$ for various instances of time at $T = 300$ K. Arrows point toward increasing time.

with k the transition rate and with the dot denoting differentiation with respect to time. As the two fractions are simply related via $\phi_\uparrow(t) + \phi_\downarrow(t) = 1$, we will from now on only focus on the fraction of jumped particles $\phi_E(t) = \phi_\downarrow(t)$, with $E \equiv -k_B T \ln(k/k_0)$ and k_0 a measure for the attempt rate. Here the subscript E stands for the activation energy of the process and has been added to differentiate $\phi_E(t)$ from the jump fraction $\phi(t)$ as measured during the MD simulation (as $\phi(t)$ does not necessarily stem from one energy barrier).

From the fraction of jumped particles we can construct the normalized autocorrelation function[56]

$$\begin{aligned} C_\phi(t) &= \frac{\langle \Delta\phi(t)\Delta\phi(0)\rangle}{\langle \Delta\phi(0)\Delta\phi(0)\rangle} \\ &= \frac{\langle [\phi_i(t) - \phi_{eq}][\phi_i(0) - \phi_{eq}]\rangle}{\langle [\phi_i(0) - \phi_{eq}][\phi_i(0) - \phi_{eq}]\rangle} \\ &= 1 - 2\langle \phi_i(t)\rangle \\ &= 1 - 2\phi(t) \end{aligned} \tag{16}$$

in which the equalities $\phi_{eq} = 1/2$ and $\phi(0) = 0$ have been used. The average $\langle \cdots \rangle$ is taken over all phenyl rings i. So in the case of a single transition rate eq 16 simplifies to $C_\phi(t) = C_{\phi E}(t) = e^{-t/\tau}$, with $\tau = 1/(2k)$.

Note that $C_\phi(t)$ is very similar to $C_\chi(t)$. In fact, if the librating motion within the local minimum would be negligible and all rings would be either at the position $\chi = \pi$ or $\chi = 0$, then $\cos[\Delta\chi(t)] = -1$ if the phenyl ring has flipped and $\cos[\Delta\chi(t)] = 1$ if it did not flip. In this case $\phi(t) = 1/2\ \langle 1 - \cos[\Delta\chi(t)]\rangle$ and hence $C_\chi(t) = C_\phi(t)$. The simulation results indicate that these two functions indeed show approximately the same long-time behavior. Fitting both $C_\chi(t)$ and $C_\phi(t)$ by a stretched exponential (eq 6) results in almost the same values for β and τ_c; the difference is less than 3% for β and 9% for τ_c for $T > T_g$. However, the short-time behavior is very different because in this regime the librating motion cannot be neglected for $C_\chi(t)$. As is shown below, the short-time response of $C_\phi(t)$ is interesting to study in more detail.

On the basis of the nonexponential decay of $C_\chi(t)$, we expect to have a distribution of local free energy barriers E with a distribution function $g(E)$. Therefore, the expression for $C_{\phi E}(t)$ needs to be averaged over all possible energy barriers, i.e.

$$C_\phi(t) = \langle C_{\phi E}(t)\rangle = \int C_{\phi E}(t)\, g(E)\, dE \tag{17}$$

It is now easy to see that in general $\langle C_{\phi E}(t)\rangle$ is not a single-exponential function. By Taylor expansion the average of $C_{\phi E}(t) = \exp(-t/\tau_E)$ over the energy distribution function, $C_\phi(t)$ can be written as a linear combination of negative moments $\langle \tau^{-n}\rangle$ of the distribution function of relaxation times $\rho(\tau)$ (this distribution follows from $g(E)$ via $\tau_E = 1/(2k_E)$. It would be much more desirable to use a simpler invariant of the energy distribution function, such as a single moment of $\rho(\tau)$. This can be done by concentrating on the short-time behavior of $\phi(t) = {}^1/_2[1 - C_\phi(t)]$ and the associated first moment $\langle \tau^{-1}\rangle$ by only taking the leading part of the Taylor expansion

$$\phi(t) = \langle \phi_E(t)\rangle = \frac{1}{2} t\langle 1/\tau\rangle + \langle O(t/\tau)^2\rangle \tag{18}$$

In Figure 9 the simulation results for $\phi(t)$ are shown for various temperatures. For sufficiently high temperatures we indeed see that $\phi(t)$ saturates toward the expected equilibrium value $\phi_{eq} = {}^1/_2$ for high values of t. For small time scales $\phi(t)$ is fitted by the linear function $t/(2\tau)$. One can observe that the deviation from linearity is only small for these time scales, suggesting that we indeed mostly probe the moment $\langle \tau^{-1}\rangle$.

Plotting $\tau_{-1} \equiv \langle \tau^{-1}\rangle^{-1}$ as a function of inverse temperature results in Figure 10. Also shown are the correlation relaxation times of $C_\phi(t)$, τ_{C_ϕ} (as determined by fitting $C_\phi(t)$ by a stretched exponential, eq 6, but now with the prefactor fixed to $A = 1$). From the differences between the curves it is clear that the method of determining the relaxation time is very important

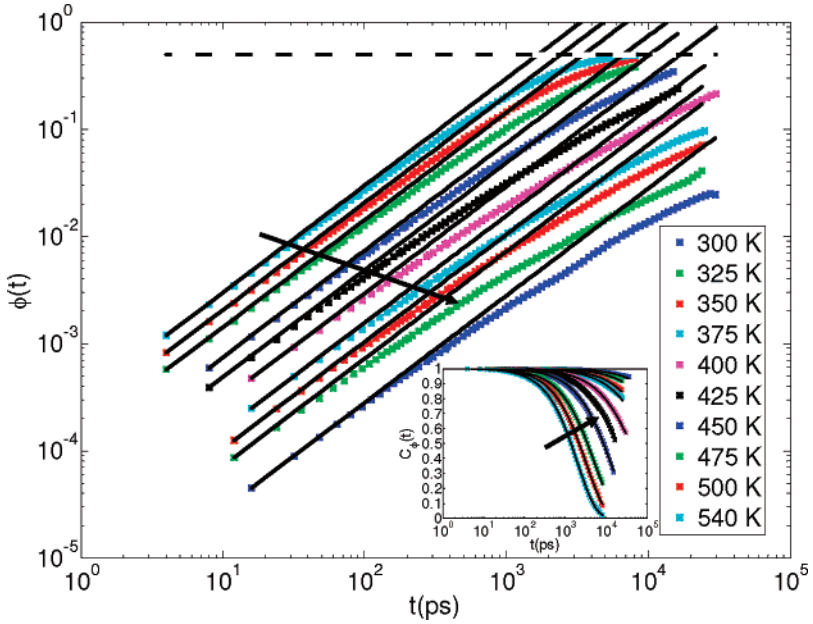

Figure 9. Fraction of phenyl rings which flipped with respect to the initial ($t = 0$) orientation. Solid lines are linear fits to the short-time behavior of the simulation data (crosses). The long time equilibrium value $\phi_{eq} = 1/2$ is shown as a dashed line. The inset shows $C_\phi(t) = 1 - 2\phi(t)$, with solid lines fits to the simulation data by a stretched exponential, eq 6, with $A = 1$. The arrows point toward decreasing temperature.

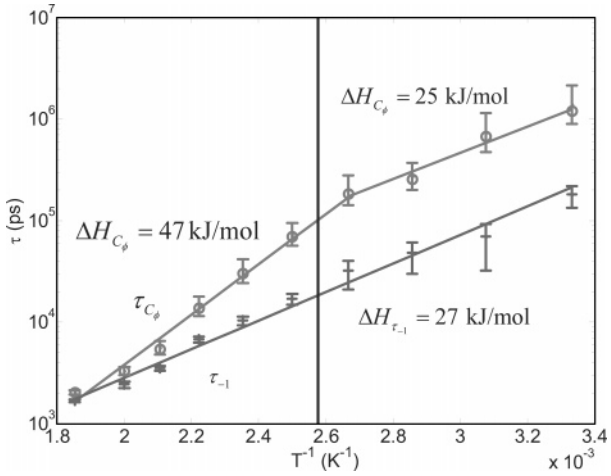

Figure 10. Typical time scales of a phenyl-ring flip as a function of the inverse temperature: (+) determined from the initial time behavior of the fraction of flipped phenyl rings $\phi(t)$; (○) determined from the correlation time of the autocorrelation function $C_\phi(t)$ (by fitting it with a stretched exponential, eq 6). The solid vertical line indicates $T_g = 388$ K. The three other solid straight lines are Arrhenius fits (12); the resulting activation enthalpies are 47 kJ mol^{-1} (○, $T \geq 375$ K), 25 kJ mol^{-1} (○, $T \leq 375$ K) and 27 kJ mol^{-1} (+). The remaining solid lines are a guide to the eye. The splitting of the two time scales τ_{-1} and τ_{C_ϕ} for lower temperatures is indicative of the broadening of the distribution of relaxation times.

for the exact temperature dependence of this time. For $T \approx 540$ K the two times as determined from the two different methods are about the same. However, for lower temperatures they start to deviate significantly from each other. A similar splitting of relaxation times upon cooling down has also been found experimentally (see, e.g., ref 57; in that review this splitting for the small molecule *o*-terphenyl is discussed). For these low temperatures in which the two time scales differ significantly from each other, the relaxation time of $C_2(t)$ becomes larger than either τ_{-1} or τ_{C_ϕ} (see Figure 5). Since $C_2(t)$ is insensitive to a phenyl ring flip, τ_{C_2} can be regarded as a measure for the time it takes for the phenyl ring to change to a new environment. So it appears that the dynamics of the phenyl ring flip become heterogeneous because this time τ_{C_2} exceeds the typical transition time of a phenyl-ring flip. Around T_g the relaxation times τ_{-1} and τ_{C_ϕ} differ by almost 1 order of magnitude. Despite this difference, they show approximately the same temperature dependence below T_g.

The observation that $\tau_{-1} \leq \tau_{C_\phi}$ can also be rationalized due to the existence of a distribution of energy barriers. Phenyl rings having a low local free energy barrier will relax first (i.e., at short times), and the phenyl rings with a higher local free energy barrier will relax later. The short-time behavior of $C_\phi(t)$ (as measured by τ_{-1}) is therefore representative for these low-energy barriers, while the long-time behavior (as measured by τ_{C_ϕ}, arising from the stretched-exponential function fit of $C_\phi(t)$) is more sensitive to the higher energy barriers. So the splitting of the two relaxation times upon cooling down can be interpreted as well as a slowing down of transitions between states with different energy barriers, thereby promoting heterogeneous dynamics.

Fitting the relaxation times τ_{-1} by an Arrhenius law results in an activation enthalpy of $\Delta H_{\tau_{-1}} = 27$ kJ mol^{-1}. Note that this enthalpy $\Delta H_{\tau_{-1}}$ is much lower than the value acquired by fitting the relaxation times of $C_\phi(t)$, 47 kJ mol^{-1} (in which the temperature range for the fit was 375−540 K), but it is remarkably close to the enthalpy barrier as determined from the temperature dependence of the distribution function of χ, viz. $\Delta H_{max} = 26$ kJ mol^{-1} (Figure 3). Note also that the activation enthalpy for $C_\phi(t)$ for temperatures below the glass-transition temperature (i.e., 300−375 K), $\Delta H_{C_\phi} = 25$ kJ mol^{-1}, is close as well to the enthalpy barrier ΔH_{max}.

The observed similarity between $\Delta H_{\tau_{-1}}$ and ΔH_{max} can also be explained by assuming a distribution of energy barriers. The free energy barrier height as determined from the distribution function is calculated using the ratio $\rho(\chi_{max})/\rho(\chi_{min})$, i.e., $\Delta G_{max} = -k_B T \ln[\rho(\chi_{max})/\rho(\chi_{min})]$. What is actually measured during a simulation run is the number of phenyl rings $n(\chi)$ which have an angle between χ and $\chi + d\chi$. Call the total number of phenyl rings N. With $n(\chi) = (1/N)\rho(\chi)\, d\chi$ it follows that $n(\chi) = \langle n_E(\chi)\rangle = N\langle\rho_E(\chi)\rangle\, d\chi = N\rho(\chi)\, d\chi$. For χ_{max} we can write

$$\rho(\chi_{max}) = \langle \rho_E(\chi_{max}) \rangle$$
$$= \langle \rho(\chi_{min}) e^{-(E(\chi_{max})-E(\chi_{min}))/(k_B T)} \rangle$$
$$= \rho(\chi_{min}) \langle e^{-(E(\chi_{max})-E(\chi_{min}))/(k_B T)} \rangle \quad (19)$$

in which it has been assumed that $\rho(\chi_{min})$ is approximately independent of the local energy barrier. Therefore

$$\Delta G_{max} = -k_B T \ln(\langle e^{-(E(\chi_{max})-E(\chi_{min}))/(k_B T)} \rangle) \quad (20)$$

Similarly, averaging the inverse transition time (given by eq 12) over the distribution of energy barriers, while assuming that $\tau'_0 = \tau_0 \exp(\Delta S_{max}/k_B)$ is approximately independent of the local energy barrier gives

$$\langle \tau^{-1} \rangle = \langle {\tau'_0}^{-1} e^{-\Delta E/(k_B T)} \rangle$$
$$= {\tau'_0}^{-1} \langle e^{-(E(\chi_{max})-E(\chi_{min}))/(k_B T)} \rangle \quad (21)$$

In other words, if the assumptions are met, $\langle \tau^{-1} \rangle$ and ΔG_{max} (and therefore also ΔH_{max}, by the usage of eq 3) probe the same invariant of the energy distribution function, and as a result they yield the same enthalpy barrier height.

The correspondence between ΔH_{C_ϕ} and ΔH_{max} for $T < T_g$ could be due to the supposed fact that the width of the distribution of energy barriers is not changing much any more in this temperature range. A similar result has been observed before by MD simulations,[15] in which the spread of activation energies for a methyl group rotation in poly(vinyl methyl ether) remains constant below the glass-transition temperature; this was also seen in experimental data on the same system. However, another reason could be the limited time window of the autocorrelation function $C_\phi(t)$. Fitting this with a stretched exponential function then effectively favors the short time scales over the long time scales, so that it becomes more sensitive to the lower energy barriers. Upon cooling further, this effect becomes even stronger.

The method of determining the time scale by means of the fraction of escaped particles at short times gives thus a relaxation time of about 30 ns at $T = 375$ K. This is consistent with NMR experiments,[58] which find that the correlation time of the π jump is in the range of 10 −100 ns at $T = 373$ K.

4. Summary, Conclusions, and Outlook

It has been shown that the effective energy barrier associated with a phenyl-ring flip of polystyrene is very dependent on the physical quantity under study. This is a result of the growth of dynamical heterogeneity upon cooling, as confirmed by various methods. For relatively high temperatures the effect is small, but close to the glass transition heterogeneity plays an important role. For temperatures just above the glass transition the activation enthalpy of one relaxation time of the phenyl-ring flip (probing the long-time behavior) is almost a factor of 2 higher than that of another relaxation time of the same process (but probing the short-time behavior), as is shown in Figure 10. Nevertheless, the fraction of flipped phenyl rings for very small times gives an estimate for the average transition rate, and it turns out that the temperature dependence of this transition rate is similar to one that would be expected from the effective energy barrier based on the probability distribution function of the orientation of the phenyl ring, despite the presence of heterogeneous dynamics.

A possible reason for the observed apparent widening of the distribution of local energy barriers upon cooling could be due to the following picture. It is known that the effective phenyl-ring barrier depends on the local environment, in particular on the backbone conformation. The flip barrier associated with some conformations can easily exceed the α-relaxation time. A phenyl ring in such a state will be able to flip faster by changing its state (by means of a change in the nearby backbone conformation) to another one with a low flip barrier. So the total time it takes to flip for such phenyl rings is on the scale of the sum of the relaxation time of the environment and the low-barrier flip time. For high temperatures the local environment relaxes much faster than the low-barrier flip time. In this case the flip time for the phenyl rings with a high flip barrier is almost the same as the flip time for phenyl rings with a low flip barrier, so that the heterogeneity in the flipping dynamics is practically absent. However, for lower temperatures the environment of the phenyl rings becomes more sluggish, and eventually the relaxation time of the environment will be much larger than the low-barrier flip time. In this case the phenyl rings with a high flip barrier will flip on a much slower time scale than the low-barrier phenyl rings. This encompasses a spread in relaxation times and therefore heterogeneous dynamics.

In contrast to temperatures above the glass transition, it turns out that for the sub-T_g regime the two different definitions of relaxation time (from a KWW fit and from the short-time analysis) render about the same effective energy barrier. This could be either due to the limited time window of the relaxation function or due to that the width of the energy distribution stays approximately constant. This energy barrier for the phenyl-ring flip is shown to be in accordance with the energy barrier for the γ-relaxation as is deduced from experimental results. Of course, this does not rigorously imply that the γ-relaxation is the result of the phenyl-ring flip. It is also possible that the phenyl ring flip acts as an indicator for the γ-relaxation but that it does not participate in the mechanical relaxation, as is also speculated for the π-flip in polycarbonate.[59] Another possibility is that the γ relaxation is due to the backbone relaxation, as preliminary results show that the free energy barrier between some conformations is of about the same magnitude as the free energy energy barrier of a phenyl-ring flip. A more stringent test would be to carry out a simulation in which the γ-relaxation is identified, such as with an oscillatory shear experiment. The persistence or disappearance of the γ-relaxation upon artificially increasing the phenyl-ring-flip barrier would then show whether this is the true molecular origin of the γ-relaxation.

References and Notes

(1) Debenedetti, P. G. *Metastable Liquids—Concepts and Principles*; Princeton University Press: Princeton, NJ, 1996.
(2) Santangelo, P. G.; Roland, C. M. *Macromolecules* **1998**, *31*, 4581−4585.
(3) Yano, O.; Wada, Y. *J. Polym. Sci., Part A-2* **1971**, *9*, 669−686.
(4) Vyazovkin, S.; Dranca, I. *J. Phys. Chem. B* **2004**, *108*, 11981−11987.
(5) Goyanes, S. N. *J. Appl. Polym. Sci.* **2000**, *75*, 865−873.
(6) Reich, S.; Eisenber, A. *J. Polym. Sci., Part A-2: Polym. Phys.* **1972**, *10*, 1397−1400.
(7) Tonelli, A. E. *Macromolecules* **1973**, *6*, 682−683.
(8) Tanabe, Y. *J. Polym. Sci., Part B: Polym. Phys.* **1985**, *23*, 601−606.
(9) Hagele, P. C.; Beck, L. *Macromolecules* **1977**, *10*, 213−215.
(10) Khare, R.; Paulaitis, M. E. *Chem. Eng. Sci.* **1994**, *49*, 2867−2879.
(11) Rapold, R. F.; Suter, U. W.; Theodorou, D. N. *Macromol. Theory Simul.* **1994**, *3*, 19−43.
(12) Khare, R.; Paulaitis, M. E. *Macromolecules* **1995**, *28*, 4495−4504.
(13) Sillescu, H. *J. Non-Cryst. Solids* **1999**, *243*, 81−108.
(14) Nicholson, T. M.; Davies, G. R. *Macromolecules* **1997**, *30*, 5501−5505.
(15) Saelee, C.; Nicholson, T. M.; Davies, G. R. *Macromolecules* **2000**, *33*, 2258−2265.

(16) Karatasos, K.; Ryckaert, J. P.; Ricciardi, R.; Laupretre, F. *Macromolecules* **2002**, *35*, 1451−1462.
(17) Jin, W. Z.; Boyd, R. H. *Polymer* **2002**, *43*, 503−507.
(18) Berthet, J. C.; Saelee, C.; Liang, T. N.; Nicholson, T. M.; Davies, G. R. *Macromolecules* **2006**, *39*, 8186−8192.
(19) Mondello, M.; Yang, H.-J.; Furuya, H.; Roe, R.-J. *Macromolecules* **1994**, *26*, 3566−3574.
(20) Furuya, H.; Mondello, M.; Yang, H. J.; Roe, R. J.; Erwin, R. W.; Han, C. C.; Smith, S. D. *Macromolecules* **1994**, *27*, 5674−5680.
(21) Roe, R. J.; Mondello, M.; Furuya, H.; Yang, H. J. *Macromolecules* **1995**, *28*, 2807−2818.
(22) Kotelyanskii, M.; Wagner, N. J.; Paulaitis, M. E. *Macromolecules* **1996**, *29*, 8497−8506.
(23) Han, J.; Boyd, R. H. *Polymer* **1996**, *37*, 1797−1804.
(24) Nyden, M. R.; Coley, T. R.; Mumby, S. *Polym. Eng. Sci.* **1997**, *37*, 1496−1500.
(25) Roe, R. *J. Non-Cryst. Solids* **1998**, *235*−*237*, 308−313.
(26) Ayyagari, C.; Bedrov, D.; Smith, G. D. *Macromolecules* **2000**, *33*, 6194−6199.
(27) Lyulin, A. V.; Michels, M. A. J. *Macromolecules* **2002**, *35*, 1463−1472.
(28) Lyulin, A. V.; Balabaev, N. K.; Michels, M. *Macromolecules* **2002**, *35*, 9595−9604.
(29) Lyulin, A. V.; Balabaev, N. K.; Michels, M. *Macromolecules* **2003**, *36*, 8574−8575.
(30) He, Y. Y.; Lutz, T. R.; Ediger, M. D.; Ayyagari, C.; Bedrov, D.; Smith, G. D. *Macromolecules* **2004**, *37*, 5032−5039.
(31) Faller, R. *Macromolecules* **2004**, *37*, 1095 −1101.
(32) Lyulin, A. V.; Vorselaars, B.; Mazo, M. A.; Balabaev, N. K.; Michels, M. A. J. *Europhys. Lett.* **2005**, *71*, 618−624.
(33) Lyulin, A. V.; Michels, M. A. J. *J. Non-Cryst. Solids* **2006**, *352*, 5008−5012.
(34) Sun, Q.; Faller, R. *Macromolecules* **2006**, *39*, 812−820.
(35) Harmandaris, V. A.; Adhikari, N. P.; van der Vegt, N. F. A.; Kremer, K. *Macromolecules* **2006**, *39*, 6708−6719.
(36) Allen, M.; Tildesley, D. *Computer Simulation of Liquids*; Clarendon Press: Oxford, UK, 1987.
(37) Lemak, A. S.; Balabaev, N. K. *J. Comput. Chem.* **1996**, *17*, 1685−1695.
(38) Zoller, P.; Walsh, D. J. *Standard Pressure-Volume-Temperature Data for Polymers*; Technomic Pub. Co.: Lancaster, PA, 1995.
(39) Rabinovich, A. L.; Ripatti, P. O.; Balabaev, N. K.; Leermakers, F. A. M. *Phys. Rev. E* **2003**, *67*, 011909.
(40) Abe, Y.; Tonelli, A. E.; Flory, P. J. *Macromolecules* **1970**, *3*, 294−303.
(41) Robyr, P.; Gan, Z.; Suter, U. W. *Macromolecules* **1998**, *31*, 8918−8923.
(42) Chandler, D. *Introduction to Modern Statistical Mechanics*; Oxford University Press: Oxford, 1987.
(43) Witten, T.; Pincus, P. A. *Structured Fluids: Polymers, Colloids, Surfactants*; Oxford University Press: New York, 2004.
(44) Lindsey, C. P.; Patterson, G. D. *J. Chem. Phys.* **1980**, *73*, 3348−3357.
(45) Smith, G. D.; Bedrov, D.; Paul, W. *J. Chem. Phys.* **2004**, *121*, 4961−4967.
(46) Lewis, L. J.; Wahnstrom, G. *Phys. Rev. E* **1994**, *50*, 3865−3877.
(47) Darinskii, A. A.; Gotlib, Y. Y.; Lyulin, A. V.; Klushin, L. I.; Neelov, I. M. *Vysokomol. Soedin. Ser. A* **1990**, *32*, 2289−2295.
(48) Fuson, M. M.; Hanser, K. H.; Ediger, M. D. *Macromolecules* **1997**, *30*, 5714−5720.
(49) Jin, Y.; Boyd, R. H. *J. Chem. Phys.* **1998**, *108*, 9912−9923.
(50) Doi, M. *Introduction to Polymer Physics*; Oxford University Press: Oxford, 1995.
(51) Bicerano, J. *J. Polym. Sci., Part B: Polym. Phys.* **1991**, *29*, 1345−1359.
(52) Hansen, J.-P.; McDonald, I. R. *Theory of Simple Liquids*, 2nd ed.; Acedemic Press: London, 1986.
(53) Brown, D.; Clarke, J. H. R. *J. Chem. Phys.* **1990**, *92*, 3062−3073.
(54) Risken, H. *The Fokker-Planck Equation—Methods of Solution and Applications*, 2nd ed.; Springer-Verlag: Berlin, 1989.
(55) Colmenero, J.; Moreno, A. J.; Alegria, A. *Prog. Polym. Sci.* **2005**, *30*, 1147−1184.
(56) Doi, M.; Edwards, S. *The Theory of Polymer Dynamics*; Clarendon Press: New York, 1986.
(57) Ediger, M. D. *Annu. Rev. Phys. Chem.* **2000**, *51*, 99−128.
(58) Spiess, H. W. *Colloid Polym. Sci.* **1983**, *261*, 193−209.
(59) Wehrle, M.; Hellmann, G. P.; Spiess, H. W. *Colloid Polym. Sci.* **1987**, *265*, 815−822.

MA070669R